Low-Frequency Analysis of Multiconductor Transmission Lines for Crosstalk Design Rules

Jesper Lansink Rotgerink, *Member, IEEE*, Harmen Schippers, *Member, IEEE*, and Frank Leferink, *Senior Member, IEEE*

***Abstract*—For early risk assessment in the design of cabling in an aircraft, as well as cable bundle optimization, efficient crosstalk estimations, and dependency of crosstalk with respect to designable parameters are required. A low-frequency technique for analyzing crosstalk in multiconductor transmission lines is presented. The result of this analysis is a closed-form expression for crosstalk in a specific cabling configuration. The technique has been validated via measurements and is used in two examples comprising two wire pairs close to a ground plane and in free space. Low-frequency closed-form expressions for near-end crosstalk are derived for both situations, which directly relate any designable parameter to crosstalk levels. Moreover, these expressions clearly show differences between the cases with and without a ground plane. Specifically, with the ground plane, the decrease in crosstalk when doubling the separation distance is 24 dB for pairs close to the ground, while it is 12 dB in free space. The closed-form expressions are utilized to create an overview of sensitivities of crosstalk to all designable parameters for both configurations. Finally, the low-frequency approximations of the chain parameters are applied to more complex nonuniform transmission lines, yielding more than 20 times faster computations when compared with complete MTL simulations.**

***Index Terms*—Closed-form solutions, crosstalk, low-frequency analysis, multiconductor transmission lines (MTLs), parameter sensitivity.**

I. Introduction

MODERN airframes and cars include numerous electric and electronic systems. This requires the routing of a great amount of cabling throughout the entire structure. Signals applied to closely spaced cables can cause electromagnetic (EM) coupling, crosstalk. This might lead to malfunction of systems that are attached to those cables when the interference level is high or when systems are highly sensitive. Tradeoffs have to be made between protection measures such as segregation of cables and the application of extra shielding on the one hand, and the extra weight the aircraft or car has to carry due to such precautions on the other hand. EM simulations can assist in making such tradeoffs. Complex, state-of-the-art solution methods are used to simulate crosstalk effects in detailed models of practical cable bundles. Several extensions of the elegant multiconductor transmission line (MTL) theory by Clayton Paul [1] facilitate, for example, in accurate simulation of twisted wire pairs [2], [3], and the inclusion of inhomogeneous insulation around conductors by numerical estimation of per-unit-length (PUL) parameters [1], [4]. Other advancements make it possible to include more complex longitudinal nonuniformities that are present in practical cable bundles, such as meandering of cables [5], [6] and twist irregularities [7], [8]. Finally, statistical methods could be considered if uncertainties in cable bundles should be taken into account [9]–[14]. Combination of the necessary state-of-the-art models could yield reliable crosstalk predictions in complex cable bundles.

However, with modern aircrafts carrying several hundred kilometers of cabling, performing such complete and accurate simulations for every possible configuration of an entire electrical wiring interconnection system (EWIS) will be a computationally huge task, even when quick simulation methods are used for the computation of a single EWIS [15]. Especially when used in the optimization of cable bundles, in which numerous realizations of cable bundles and routing scenarios should be analysed, more efficient methods are useful to reduce the solution space. Therefore, the effective application of electromagnetic compatibility (EMC) design rules for cable routing is important, since these allow early identification of possible risks. The dependencies of crosstalk on designable parameters such as separation distances are essential for such design rules. Designable parameters are those of which the values can be changed by the design engineer. A quick analysis of the entire EWIS based upon such design rules can yield both routing for low-risk signals and EMC bottle-necks for the high-risk signals. Subsequent design stages could then involve an accurate assessment of the routing of these high-risk signals. The desired design rules can be obtained by simplified crosstalk expressions as a result of the lossless and low-frequency analysis of the MTL. Crosstalk for low frequencies, or electrically short lines, in a lossless case, can quickly be computed by Spice simulations. However, these do not result in clear dependencies of crosstalk with respect to designable parameters. Alternatively, circuit analysis of lossless and

Manuscript received May 1, 2018; revised July 27, 2018; accepted August 27, 2018. Date of publication September 17, 2018; date of current version September 30, 2019. This work was supported by GKN Fokker Elmo, the Netherlands. *(Corresponding author: Jesper H. G. J. Lansink Rotgerink.)*

J. L. Rotgerink is with the Netherlands Aerospace Centre, Marknesse 8316 PR, The Netherlands, and also with the Telecommunication Engineering Group, University of Twente, Enschede 7522 NB, The Netherlands (e-mail: Jesper.Lansink.Rotgerink@nlr.nl).

H. Schippers is with the Netherlands Aerospace Centre, Marknesse 8316 PR, The Netherlands (e-mail: Harmen.Schippers@nlr.nl).

F. Leferink is with the Telecommunication Engineering Group, University of Twente, Enschede 7522 NB, The Netherlands, and also with the Thales Nederland B.V., Hengelo 7554 RR, The Netherlands (e-mail: leferink@ieee.org).

Color versions of one or more of the figures in this paper are available online at http://ieeexplore.ieee.org.

Digital Object Identifier 10.1109/TEMC.2018.2868985

0018-9375 © 2018 IEEE. Personal use is permitted, but republication/redistribution requires IEEE permission.
See http://www.ieee.org/publications_standards/publications/rights/index.html for more information.

Authorized licensed use limited to: Technical Activities Board. Downloaded on June 23,2020 at 15:17:24 UTC from IEEE Xplore. Restrictions apply.

electrically short transmission lines is often used to obtain analytic crosstalk expressions. For instance, white derives expressions for the coupling between two single wires above ground [16], and in [17] and [18], Paul also derives similar expressions for crosstalk between a single wire and a twisted pair or a shielded wire above ground. However, circuit analysis becomes tedious for more than 2 or 3 wires above a ground plane, and therefore there is a lack of such analytic expressions in the literature.

In this paper, we present a mathematical method to derive simplified but efficient closed-form crosstalk expressions directly from the matrix formulations of the MTL equations. These expressions directly relate crosstalk to all designable parameters and can be used for design rules to make early decisions about routing and segregation of low-risk signals. Application of this method yields such crosstalk expressions for four and five-conductor transmission lines involving wire pairs 1) in free space and 2) above a perfectly conducting ground plane. The first application of this method, published in [19], showed fourth-order dependence with respect to separation distance for crosstalk between wire pairs close to a perfectly conducting ground plane. In this paper, the method is also applied to crosstalk between wire pairs where a ground plane is absent. The derived closed-form expressions for both situations clearly show the differences in dependencies of crosstalk on all designable parameters. Finally, it is also shown that the set of low-frequency equations that form the basis of the presented methodology is very useful for a quick, lossless crosstalk analysis of more complex and nonuniform MTLs. A speedup of more than 20 times is reached when compared with the global MTL method. The methods and expressions in this paper also form an efficient candidate for multiple run optimization of an entire EWIS.

Section II of this paper presents the mathematical context of the proposed low-frequency method. In Section III, two examples are given, comprising two wire pairs 1) close to a perfect ground plane and 2) in free space. Closed-form expressions are derived and used for the analysis of parameter sensitivity. The final section presents the conclusions.

II. Methodology

This section describes the mathematical analysis that leads to closed-form expressions for crosstalk. Consider an MTL with $n + 1$ conductors, including a reference conductor. Let $\mathbf{V_0}$ denote the vector containing the voltages at the near-end of the n nonreference conductors with respect to the reference. Corresponding currents are represented by $\mathbf{I_0}$. Since crosstalk is defined as the ratio of voltage induced in a receptor or victim transmission line, over that in the generator or culprit line, the near-end crosstalk (NEXT) γ_{NE} can be expressed by

$$\gamma_{\mathrm{NE}} = \frac{\mathbf{U}_2^T \mathbf{V}_0}{\mathbf{U}_1^T \mathbf{V}_0}. \tag{1}$$

Here, $\mathbf{U}_1$ and $\mathbf{U}_2$ are the n-dimensional vectors that select the necessary voltages from $\mathbf{V_0}$ to obtain either common-mode or differential-mode voltages of victim and culprit in the numerator and denominator of (1), respectively.

To obtain closed-form near-end crosstalk expressions, the vector of voltages at near-end is required. For far-end crosstalk (FEXT) the far-end voltage is used in (1), but the analysis is completely similar. Therefore, in this paper, we discuss only NEXT. For the analysis of MTLs, matrix equations are presented in [1]. One way of solving these MTL equations involves the use of chain parameter matrices Φ. Suppose that the terminations of the MTL can be represented by a Thévenin equivalent, then the boundary condition for the near-end voltages is expressed as follows:

$$\mathbf{V}_0 = \mathbf{V}_S - \mathbf{Z}_S \mathbf{I}_0. \tag{2}$$

Here, $\mathbf{V_S}$ is the vector of voltage sources at the near-end side, and the termination networks at the near and far-end sides are represented by the impedance matrices $\mathbf{Z}_S$ and $\mathbf{Z}_L$. In this case, the desired voltages can be obtained by solving the corresponding currents from

$$\begin{aligned} \mathbf{A}\mathbf{I}_0 &= \left[\Phi_{11} - \mathbf{Z}_L \Phi_{21}\right] \mathbf{V}_S - \mathbf{V}_L \\ \mathbf{A} &= \left[\Phi_{11}\mathbf{Z}_S + \mathbf{Z}_L \Phi_{22} - \Phi_{12} - \mathbf{Z}_L \Phi_{21} \mathbf{Z}_S\right] \end{aligned} \tag{3}$$

and substituting $\mathbf{I_0}$ into (2). For crosstalk analysis, we assume the presence of one voltage source at the near-end side, implying

$$\mathbf{V_S} = V_S \mathbf{U}_1, \qquad \mathbf{V}_L = \mathbf{0} \tag{4}$$

in which V_S controls the magnitude of the voltage source.

Alternatively, suppose that the terminations are given by a Norton equivalent representation. Therefore, the terminations are represented by admittance matrices $\mathbf{Y}_S$ and $\mathbf{Y}_L$ on source and load side. Then the near-end voltages can be solved from

$$\begin{aligned} \mathbf{A}\mathbf{V}_0 &= \left[\Phi_{22} - \mathbf{Y}_L \Phi_{12}\right] \mathbf{I}_S + \mathbf{I}_L \\ \mathbf{A} &= \left[\Phi_{22}\mathbf{Y}_S + \mathbf{Y}_L \Phi_{11} - \Phi_{21} - \mathbf{Y}_L \Phi_{12} \mathbf{Y}_S\right]. \end{aligned} \tag{5}$$

For crosstalk analysis, we now assume one current source at the near-end side, implying

$$\mathbf{I_S} = I_S \mathbf{U}_1, \qquad \mathbf{I}_L = \mathbf{0} \tag{6}$$

in which I_S controls the magnitude of the current source.

A. Low-Frequency Approximations

Expressions that clearly give relations between crosstalk and designable parameters can be obtained by using low-frequency approximations. Such approximations are usually accurate up to frequencies at which the electrical length of the transmission line is short with respect to the wavelength of the transmitted signals. At such frequencies, the chain parameters can be approximated by

$$\begin{aligned} \Phi_{11} &= \Phi_{22} = \mathbf{I}_n \\ \Phi_{12} &= -j\omega\ell\mathbf{L} - \ell\mathbf{R} \\ \Phi_{21} &= -j\omega\ell\mathbf{C} - \ell\mathbf{G} \end{aligned} \tag{7}$$

where $\mathbf{I}_n$ is the n-dimensional identity matrix, ω is the angular frequency of the signal traveling down the transmission line,

Authorized licensed use limited to: Technical Activities Board. Downloaded on June 23,2020 at 15:17:24 UTC from IEEE Xplore. Restrictions apply.

and ℓ the length of the line. The PUL inductance and capacitance matrices are given by $\mathbf{L}$ and $\mathbf{C}$. Conductor losses can be included in the resistance matrix $\mathbf{R}$. However, by the low-frequency technique presented in this paper the high-frequency effects of conductor losses to crosstalk will be neglected. Low-frequency effects of common-impedance coupling can be derived in a way similar to how inductive and capacitive coupling will be computed for the cases in Section III of this paper. However, these examples consider crosstalk between wire pairs in which case there is no common return conductor. Therefore, in this paper, we neglect both conductor losses and losses in dielectric media, by which $\mathbf{R} = \mathbf{G} = \mathbf{0}$. Moreover, the analysis in this paper presumes weak coupling. Therefore, the usually small secondary coupling effects, as well as proximity effects, which are small whenever the wires of a wire pair are separated by isolation, are both neglected.

Substitution of (7) in (3) or (5) gives the basis for the low-frequency crosstalk analysis. The matrix inversion of $\mathbf{A}$, needed for the computation of voltages in all conductors, can be approximated by a Taylor expansion for low frequencies. Therefore, $\mathbf{A}$ is manipulated to be in the following form

$$\mathbf{A} = \mathbf{I}_n + j\omega\ell\mathbf{B}.$$

Here, for the Thévenin representation $\mathbf{B}$ follows from the substitution of (7) into (3) and multiplication by $\tilde{\mathbf{Z}} = [\mathbf{Z}_S + \mathbf{Z}_L]^{-1}$. For the Norton representation, we multiply by $\tilde{\mathbf{Y}} = [\mathbf{Y}_S + \mathbf{Y}_L]^{-1}$ after substitution of (7) into (5). For all frequencies such that $\omega\ell\|\mathbf{B}\| \ll 1$, which usually holds for electrically short lines, the inversion is then approximated by

$$\mathbf{A}^{-1} \approx \mathbf{I}_n - j\omega\ell\mathbf{B}. \tag{8}$$

We apply this operation to (3) [after substitution of (7)] to obtain the vector of currents at the near-end side. The vector of near-end voltages is then computed by (2), resulting in

$$\mathbf{V}_0 \approx V_s\mathbf{U}_1 - V_s\mathbf{Z}_S\tilde{\mathbf{Z}}\mathbf{U}_1 + j\omega\ell V_s\mathbf{Z}_S\left[\tilde{\mathbf{Z}}\mathbf{L}\tilde{\mathbf{Z}} + \tilde{\mathbf{Z}}\mathbf{Z}_L\mathbf{C}\mathbf{Z}_S\tilde{\mathbf{Z}} - \tilde{\mathbf{Z}}\mathbf{Z}_L\mathbf{C}\right]\mathbf{U}_1. \tag{9}$$

If the termination networks on both sides of the transmission line are equal, i.e., $\mathbf{Z_S} = \mathbf{Z_L} = \mathbf{Z}$, then (9) simplifies to

$$\mathbf{V}_0 \approx \frac{V_s}{2}\left[\mathbf{I}_n + \frac{1}{2}j\omega\ell\left(\mathbf{L}\mathbf{Z}^{-1} - \mathbf{Z}\mathbf{C}\right)\right]\mathbf{U}_1. \tag{10}$$

Similarly, for the Norton equivalent representation the Taylor approximation is applied to (5) to obtain the vector of voltages at the near-end side

$$\mathbf{V}_0 \approx I_s\tilde{\mathbf{Y}}\mathbf{U}_1 + j\omega\ell I_s\left[\tilde{\mathbf{Y}}\mathbf{Y}_L\mathbf{L} - \tilde{\mathbf{Y}}\mathbf{C}\tilde{\mathbf{Y}} - \tilde{\mathbf{Y}}\mathbf{Y}_L\mathbf{L}\mathbf{Y}_S\tilde{\mathbf{Y}}\right]\mathbf{U}_1. \tag{11}$$

Again, if the terminations on both sides of the transmission line are equal, i.e., $\mathbf{Y_S} = \mathbf{Y_L} = \mathbf{Y}$, then (11) simplifies to

$$\mathbf{V}_0 \approx \frac{I_s}{2}\left[\mathbf{Y}^{-1} + \frac{1}{2}j\omega\ell\left(\mathbf{L} - \mathbf{Y}^{-1}\mathbf{C}\mathbf{Y}^{-1}\right)\right]\mathbf{U}_1. \tag{12}$$

Once the vector of voltages in each conductor has been obtained, (1) is applied to compute the resulting crosstalk.

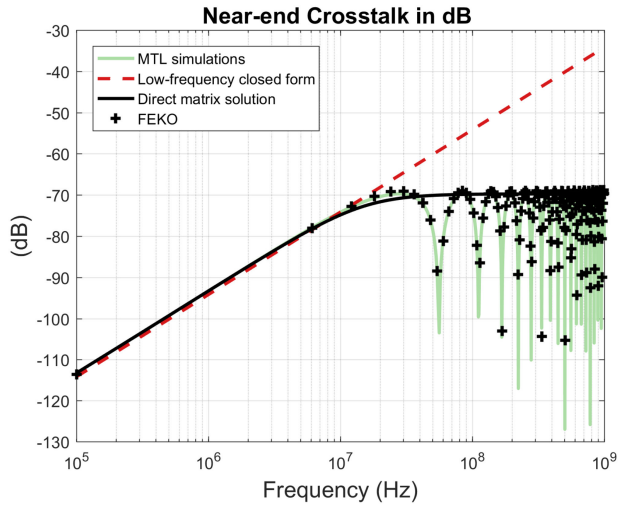

Fig. 1. MTL (green) and FEKO (black crosses) simulations of NEXT between two wire pairs above an infinite ground plane (see Section III-A). The red dashed line shows the low-frequency approximation. The black line is the direct solution found from Paul's matrix equation, given by (3), after substitution of (7).

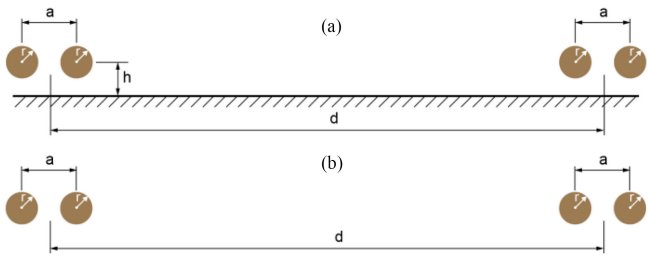

Fig. 2. Illustration of the cross sections for cabling configurations with (a) two wire pairs close to an infinite, perfectly conducting ground plane and (b) two wire pairs in free space.

Fig. 1 gives an example of the near-end crosstalk computed between two 1.9 m long wire pairs with 20 mm separation, situated parallel at a distance of 1.5 mm from an infinite ground plane, as shown by the cross section in Fig. 2(a). The values for all other parameters are given in [19] (and equal to those given later in Section III-A). The results in the figure show that by complete MTL simulation or full-wave FEKO simulation a detailed description of crosstalk in the frequency domain can be obtained. In the MTL simulations, analytic and exact expressions for the chain parameter matrices are used, including all coupling and propagation effects in all conductors. Full-wave simulations take into account all EM interactions, but are much more extensive to set up. By substituting the low-frequency approximations for Φ in (7), direct solution of (3) yields a curve in which resonances disappeared, but the trends of crosstalk behavior in the frequency domain are still present (black line). The red dashed curve represents the low-frequency approximations as result of the analysis in this paper, which does not give an exact solution for crosstalk behavior, but is perfect for determining relations to all designable parameters.

III. Application of the Presented Method

In this section, for two situations closed-form expressions are derived. In [19], the presented methodology was applied to two

Authorized licensed use limited to: Technical Activities Board. Downloaded on June 23,2020 at 15:17:24 UTC from IEEE Xplore. Restrictions apply.

single wires above a ground plane. This provided results that are widely reported in the literature. In this paper, the analysis is applied to crosstalk between wire pairs parallel and close to a ground plane, as well as without a ground plane. For both cases, first a general crosstalk expression is presented, after which leading-order dependency on designable parameters is derived with Taylor expansions after some extra assumptions.

A. Two Wire Pairs Above a Perfectly Conducting Ground Plane

Consider the cross section in Fig. 2(a), comprising two wire pairs parallel to a ground plane. The wires are numbered 1–4 from left to right and a differential voltage source is included in the termination of the first pair; differential-mode crosstalk results. The pairs are separated by a distance *d* and all wires are at equal heights *h* above the ground plane and of radius *r*. The wires in both pairs have an intrapair separation distance *a*.

1) Terminations: The terminations for the wire pairs are equal to those used in [19]. Norton equivalent representation techniques can be used to obtain the corresponding termination matrices

$$\mathbf{Z}_T = \begin{bmatrix} \mathbf{Z}^*_{cT} & \mathbf{0} \\ \mathbf{0} & \mathbf{Z}^*_{vT} \end{bmatrix}$$

$$\mathbf{Z}^*_{mT} = R_{d,mT} \begin{bmatrix} c_{mT}+\kappa_{mT} & c_{mT}-\kappa_{mT} \\ c_{mT}-\kappa_{mT} & c_{mT}+\kappa_{mT} \end{bmatrix}, m \in \{c, v\} \tag{13}$$

where subscripts v and c represent the victim or the culprit, $\kappa_{mT} = [2(R_{d,mT}/R_{c,mT}+2)]^{-1}$, $c_{mT} = [R_{d,mT}(R_{d,mT}/R_{c,mT}+2)/R_{c,mT}]^{-1} + \kappa_{mT}$ and the subscript $T \in \{S, L\}$ indicates the termination on the source or load side. The variable $R_{d,mT}$ is the differential-mode and $R_{c,mT}$ the common-mode termination of either culprit or victim wire pair at the load or source side. The common-mode impedance $R_{c,mT}$ is present if the wire pair is also connected to ground via a certain impedance. In our measurements, wire pairs are always connected to ground via a balun with known impedance. Finally, since a differential source was added to the culprit line, we define $\mathbf{U}_1 = (-1, 1, 0, 0)^T$ and $\mathbf{U}_2 = (0, 0, -1, 1)^T$. By (4), this implies that a voltage difference of $2V_S$ is set and maintained.

2) Near-End Crosstalk: The given termination matrices (9) can be used to compute the numerator and denominator of (1)

$$\mathbf{U}_1^T \mathbf{V}_0 \approx \frac{2V_S R_{d,cL}\kappa_{cL}}{R_{d,cL}\kappa_{cL} + R_{d,cS}\kappa_{cS}}$$

$$\mathbf{U}_2^T \mathbf{V}_0 \approx \frac{j\omega\ell V_S R_{d,vS}\kappa_{vS}\left(l_{13}+l_{24}-(l_{14}+l_{23})\right)}{2\left(R_{d,cL}\kappa_{cL}+R_{d,cS}\kappa_{cS}\right)\left(R_{d,vL}\kappa_{vL}+R_{d,vS}\kappa_{vS}\right)} - \frac{2j\omega\ell V_S R_{d,cL}R_{d,vL}R_{d,vS}\kappa_{cL}\kappa_{vL}\kappa_{vS}\left(c_{13}+c_{24}-(c_{14}+c_{23})\right)}{(R_{d,cL}\kappa_{cL}+R_{d,cS}\kappa_{cS})(R_{d,vL}\kappa_{vL}+R_{d,vS}\kappa_{vS})}. \tag{14}$$

Here, l_{ij} and c_{ij} are elements of the inductance and capacitance matrices. These can be computed by for instance the analytic expressions in [1], or numerical methods [4]. Substituting (14) into (1) results in the following expressions for capacitive crosstalk:

$$\gamma_{\mathrm{NE,cap}} \approx j\omega\ell \frac{R_{vL}R_{vS}\kappa_{vL}\kappa_{vS}\left(c_{14}+c_{23}-c_{13}-c_{24}\right)}{\left(R_{vL}\kappa_{vL}+R_{vS}\kappa_{vS}\right)} \tag{15}$$

and inductive crosstalk

$$\gamma_{\mathrm{NE,ind}} \approx j\omega\ell \frac{R_{vS}\kappa_{vS}\left(l_{13}-l_{14}-l_{23}+l_{24}\right)}{4R_{cL}\kappa_{cL}\left(R_{vL}\kappa_{vL}+R_{vS}\kappa_{vS}\right)}. \tag{16}$$

In Section III-A-3, Taylor expansions of the analytical PUL parameters will be used to obtain the leading order, closed-form crosstalk expressions.

3) Closed-Form Crosstalk Expression: PUL parameters characterize the transmission line. We use Taylor expansions combined with the nice structure of inductance and capacitance matrices to derive our low-frequency closed-form expressions for crosstalk. The medium surrounding the wires is assumed to be homogeneous. Material properties are given by $\varepsilon = \varepsilon_r\varepsilon_0$ and $\mu = \mu_r\mu_0$, where the subscripts *r* and *0* indicate relative and free-space permittivity or permeability, respectively. Following Paul's analytical expressions for cylindrical conductors [1], the induction matrix for the current example is equal to

$$\mathbf{L} = \begin{bmatrix} \mathbf{L}_{000} & \mathbf{L}_{12} \\ \mathbf{L}_{12}^T & \mathbf{L}_{000} \end{bmatrix} \tag{17}$$

where $\mathbf{L_{000}}$ represents the inductance within a pair, given by

$$\mathbf{L}_{000} = \beta \begin{bmatrix} \ln(2h/r) & \ln\sqrt{1+y} \\ \ln\sqrt{1+y} & \ln(2h/r) \end{bmatrix} \tag{18}$$

where $\beta = \mu/2\pi$ and $y = 4h^2/a^2$. The mutual inductance between the pairs equals

$$\mathbf{L}_{12} = \frac{\beta}{2} \begin{bmatrix} \ln(1+x) & \ln\left(1+\frac{x}{(1+\alpha)^2}\right) \\ \ln\left(1+\frac{x}{(1-\alpha)^2}\right) & \ln(1+x) \end{bmatrix}$$

where $\alpha = a/d$ and $x = 4h^2/d^2$. Suppose α is a small parameter, i.e., $a \ll d$. Then the inversion of $\mathbf{L}$, which is necessary for the computation of the capacitance matrix, can be approximated by Taylor expansions. Therefore, first $\mathbf{L_{12}}$ is expanded in terms of α

$$\hat{\mathbf{L}}_{12} = \underbrace{\begin{bmatrix} 1 & 1 \\ 1 & 1 \end{bmatrix}}_{\mathbf{L}_{01}} b + \underbrace{\begin{bmatrix} 0 & -1 \\ 1 & 0 \end{bmatrix} \frac{\beta x}{x+1}}_{\mathbf{L}_1} \alpha + \underbrace{\begin{bmatrix} 0 & 1 \\ 1 & 0 \end{bmatrix} \frac{\beta}{2} \frac{3x+x^2}{(x+1)^2}}_{\mathbf{L}_2} \alpha^2 \tag{19}$$

where $b = \beta/2 \cdot \ln(1+x)$. The hat notation is used for Taylor approximations. Substituting (19) into (17) yields a second-order Taylor approximation for $\mathbf{L}$

$$\hat{\mathbf{L}} = \underbrace{\mathbf{L}_{00} + \mathbf{L}_{01} \cdot b}_{\mathbf{L}_0} + \mathbf{L}_1\alpha + \mathbf{L}_2\alpha^2$$

$$\mathbf{L}_{00} = \begin{bmatrix} \mathbf{L}_{000} & \mathbf{0} \\ \mathbf{0} & \mathbf{L}_{000} \end{bmatrix}. \tag{20}$$

Authorized licensed use limited to: Technical Activities Board. Downloaded on June 23,2020 at 15:17:24 UTC from IEEE Xplore. Restrictions apply.

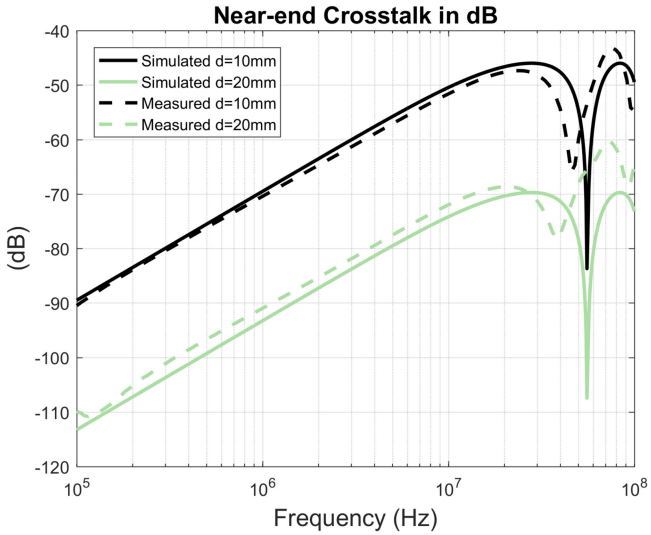

Fig. 3. MTL simulations and measurements of NEXT for two separation distances in the wire configuration given in Fig. 2(a).

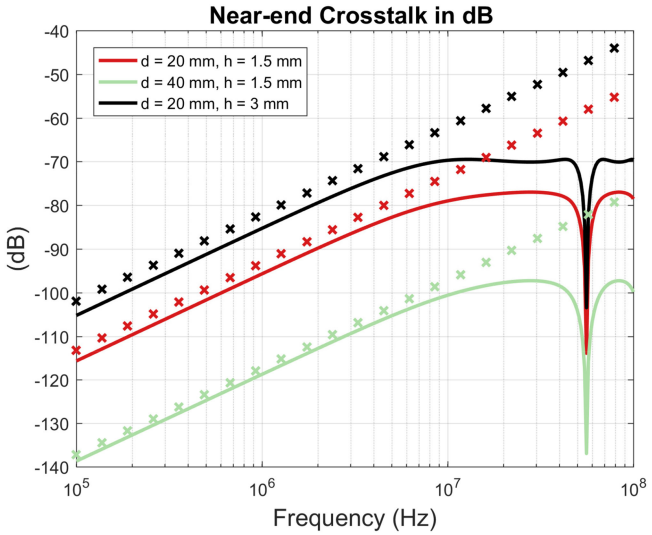

Fig. 4. MTL simulations (solid lines) and closed-form expressions (24) (crosses) of NEXT three different cases of the wire configuration given in Fig. 2(a), in which 4 terminated wires are included in between the wire pairs.

This second-order polynomial form for the inductance matrix can be utilized to compute the inverse of $\mathbf{L}$ by the Taylor expansion of a quadratic polynomial. This is applied to determine the capacitance matrix

$$\hat{\mathbf{C}} \approx \mu\varepsilon \left[\mathbf{I}_4 - \mathbf{L}_0^{-1}\mathbf{L}_1\alpha - \left(\mathbf{L}_0^{-1}\mathbf{L}_2 - \mathbf{L}_0^{-1}\mathbf{L}_1\mathbf{L}_0^{-1}\mathbf{L}_1\right)\alpha^2\right]\mathbf{L}_0^{-1}. \tag{21}$$

Finally, the inverse of $\mathbf{L_0}$ has to be determined. Suppose that the wire pairs are close to the reference ground plane than to each other $(h < d/2\sqrt{2})$, by which $x \ll 1$ and thus $b \ll 1$. In that case

$$\hat{\mathbf{L}}_0^{-1} = [\mathbf{I}_4 - \mathbf{L}_{00}^{-1}\mathbf{L}_{01} \cdot b]\mathbf{L}_{00}^{-1}.$$

The structure of inductance and capacitance matrices is utilized to obtain the final closed-form expression for the near-end crosstalk between two wire pairs close to the ground. For presentation purpose, suppose that $\mathbf{Z_S} = \mathbf{Z_L} = \mathbf{Z}$ (subscript *S/L* is dropped for $R_{d,mT}$). Combining (15) and (16), (20) and (21) then leads to closed-form expressions for inductive crosstalk

$$\gamma_{\mathrm{NE,ind}} \approx \frac{-3\mu}{2\pi R_{d,c}}\left(\frac{R_{d,c}}{R_{c,c}} + 2\right)a^2h^2j\omega l d^{-4} \tag{22}$$

and capacitive crosstalk

$$\gamma_{\mathrm{NE,cap}} \approx \frac{-24\pi\varepsilon R_{d,v}}{\left(\frac{R_{d,v}}{R_{c,v}} + 2\right)}\frac{a^2h^2j\omega l d^{-4}}{\ln^2\left(r^2\left(\frac{1}{4h^2} + \frac{1}{a^2}\right)\right)}. \tag{23}$$

The total NEXT follows from the addition of the inductive and capacitive expressions

$$\gamma_{\mathrm{NE}} \approx \gamma_{\mathrm{NE,ind}} + \gamma_{\mathrm{NE,cap}}. \tag{24}$$

The dependencies on all designable parameters are clearly shown in (22) and (23). The fourth-order dependency on wire pair separation is important. It implies that when d is doubled, the crosstalk decreases by 24 dB. For most other wiring configurations this would be 12 dB. This fourth-order dependency is validated by the results shown in Fig. 3, which shows both MTL simulations and measurements of crosstalk between two wire pairs with a length of 1.9 m. Crosstalk levels are shown for two separation distances, namely 10 and 20 mm. Values for other parameters are: $a = 2.5$ mm, $r = 0.49$ mm, $h = 1.5$ mm, $\varepsilon_r = 2$, $R_{\mathrm{d,c}} = R_{\mathrm{d,v}} = 112.5\ \Omega$, and $R_{\mathrm{c,c}} = R_{\mathrm{c,v}} = 450\ \Omega$ (equal load and source side terminations). Indeed, in both measurements and simulations, the difference between the results for the two separations is approximately 24 dB. Moreover, the measured crosstalk results agree with those from MTL simulations. Finally, Fig. 4 shows similar results of MTL simulations and closed-form expressions for the case where four extra wires, terminated with 50 Ω to ground, are arbitrarily placed in between the two wire pairs. Three variations of the parameters d and h are shown, while other parameters are equal to those presented before. Simulated results illustrate that extra conductors slightly affect the levels of crosstalk, but the parameter dependencies roughly remain the same. Situations with other terminations show that it is actually only the capacitive coupling between the wire pairs that are influenced by nearby conductors.

The measurements were performed between two wire pairs that were fixed to the given distances along the entire length of the cables by using molds of rohacell foam (see Fig. 5 for pictures of the setup). Moreover, in the case that includes a ground plane foam spacers were used to keep the wires at a fixed height above ground. The aluminum ground plane had a width of 1 m, which is enough to avoid edge effects. Baluns were used to connect the balanced pairs to the unbalanced coaxes that are connected to the measurement equipment. The frequency dependent transmission of these baluns is calibrated from the measurement results. The frequencies for which results are shown in this paper are determined by the applicability of these baluns. This frequency band includes the only little effect of ohmic and dielectric losses.

Authorized licensed use limited to: Technical Activities Board. Downloaded on June 23,2020 at 15:17:24 UTC from IEEE Xplore. Restrictions apply.

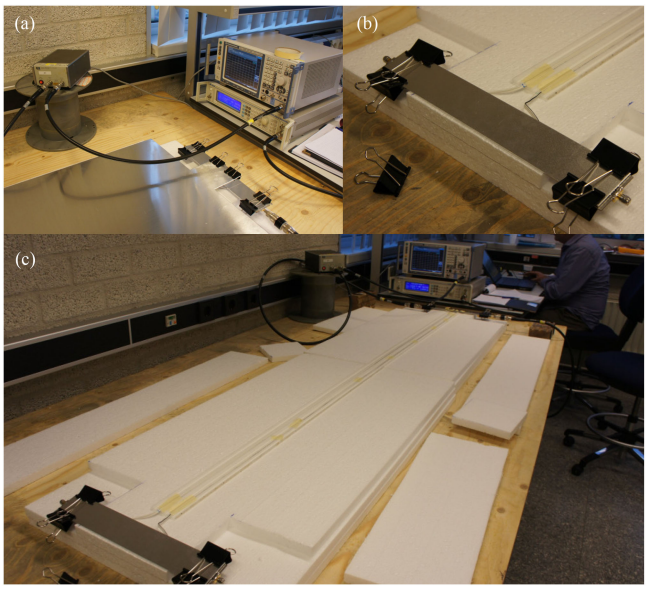

Fig. 5. Pictures of the crosstalk measurement setup. (a) Measurement equipment: Spectrum analyser, generator, and preamplifier. (b) At the end of the transmission line wire pairs are separated and soldered to balun boards that are attached to the backside of the metallic strip. (c) Foam spacers are used to keep the wire pairs at fixed separation distances and heights above ground plane along the transmission line length.

B. Two Wire Pairs in Free Space

As a second example, consider the previous configuration without a ground plane. An illustration of the cross section of this case is shown in Fig. 2(b). All properties remain the same, including the termination impedances. However, in this case, the fourth wire is taken as the reference. The other victim wire is numbered 1, and we finish by labeling the culprit wires 2 and 3. Impedance matrices $\mathbf{Z_S}$ and $\mathbf{Z_L}$ can be derived similar to the previous section (not shown here). Finally, a differential voltage source is included in the culprit pair, by which we can define $\mathbf{U}_1 = (0,-1,1)^T$ and $\mathbf{U}_2 = (1,0,0)^T$.

1) Near-End Crosstalk: Again (9) is used to compute the numerator and denominator of (1) for this wiring configuration

$$\mathbf{U}_1^T\mathbf{V}_0 \approx \frac{-2V_S\left(\bar{Y}_{cS}+2\bar{\kappa}_{cS}\right)}{\bar{Y}_{cL}+\bar{Y}_{cS}+2\bar{\kappa}_{cL}+2\bar{\kappa}_{cS}}$$

$$\mathbf{U}_2^T\mathbf{V}_0 \approx$$

$$\frac{j\omega l V_S\left(\bar{Y}_{cL}+2\bar{\kappa}_{cL}\right)\left(\bar{Y}_{cS}+2\bar{\kappa}_{cS}\right)\left(\bar{Y}_{vL}+2\bar{\kappa}_{vL}\right)(l_{12}-l_{13})}{2\left(\bar{Y}_{cL}+\bar{Y}_{cS}+2\bar{\kappa}_{cL}+2\bar{\kappa}_{cS}\right)\left(\bar{Y}_{vL}+\bar{Y}_{vS}+2\bar{\kappa}_{vL}+2\bar{\kappa}_{vS}\right)}$$

$$+\frac{4j\omega l V_S\left(\bar{Y}_{cS}+2\bar{\kappa}_{cS}\right)(2c_{12}-2c_{13}+c_{22}-c_{33})}{2\left(\bar{Y}_{cL}+\bar{Y}_{cS}+2\bar{\kappa}_{cL}+2\bar{\kappa}_{cS}\right)\left(\bar{Y}_{vL}+\bar{Y}_{vS}+2\bar{\kappa}_{vL}+2\bar{\kappa}_{vS}\right)}.$$

Here, $\bar{Y}_{mT} = R_{d,mT}^{-1}$ and $\bar{\kappa}_{mT} = (4R_{c,mT})^{-1}$ are entries from the admittance matrices, in which again the subscript *m* is either culprit or victim, and *T* denotes either load or source side. Substituting this into (1) yields the following expressions for capacitive and inductive near-end crosstalk:

$$\gamma_{\mathrm{NE,cap}} \approx j\omega\ell\frac{2c_{12}-2c_{13}+c_{22}-c_{33}}{4\left(\bar{Y}_{vL}+\bar{Y}_{vS}+2\bar{\kappa}_{vL}+2\bar{\kappa}_{vS}\right)}$$

$$\gamma_{\mathrm{NE,ind}} \approx j\omega\ell\frac{\left(\bar{Y}_{cL}+2\bar{\kappa}_{cL}\right)\left(\bar{Y}_{vL}+2\bar{\kappa}_{vL}\right)(l_{13}-l_{12})}{\left(\bar{Y}_{vL}+\bar{Y}_{vS}+2\bar{\kappa}_{vL}+2\bar{\kappa}_{vS}\right)}. \tag{25}$$

2) Closed-Form Crosstalk Expression: Following Paul's expressions for inductance between cylindrical conductors in free space, the inductance matrix for this case equals

$$\mathbf{L} = \mathbf{L}_0 + \mathbf{L}_\alpha$$

$$\mathbf{L}_0 = \begin{bmatrix}2&1&1\\1&2&1\\1&1&2\end{bmatrix}p + \begin{bmatrix}0&0&0\\0&-1&-1\\0&-1&-1\end{bmatrix}q$$

$$\mathbf{L}_\alpha = \begin{bmatrix}0&-\beta\ln(1-\alpha)&\beta\ln(1+\alpha)\\-\beta\ln(1-\alpha)&0&\beta\ln(1+\alpha)\\\beta\ln(1+\alpha)&\beta\ln(1+\alpha)&2\beta\ln(1+\alpha)\end{bmatrix} \tag{26}$$

where $p = \beta\ln(a/r)$ and $q(d) = 2\beta\ln(a/d)$. Taylor expansion of the inductance matrix with respect to the small parameter α leads to

$$\hat{\mathbf{L}}_1 = \mathbf{L}_1\cdot\alpha + \mathbf{L}_2\cdot\alpha^2$$

$$= \begin{bmatrix}0&1&1\\1&0&1\\1&1&2\end{bmatrix}\cdot\beta\cdot\alpha + \begin{bmatrix}0&1&-1\\1&0&-1\\-1&-1&-2\end{bmatrix}\cdot\frac{\beta}{2}\cdot\alpha^2. \tag{27}$$

The capacitance matrix is approximated as before by (21). The inverse of $\mathbf{L_0}$ has to be calculated explicitly in terms of *p* and *q*, since it cannot be expressed in terms of a small parameter

$$\mathbf{L}_0^{-1} = \frac{1}{4(p-q)}\begin{bmatrix}3-2g&-1&-1\\-1&3-2g&-1+2g\\-1&-1+2g&3-2g\end{bmatrix}$$

where $g = q/p$. The above-mentioned approximations for the capacitance and inductance matrices can be used to obtain a closed-form expression for near-end crosstalk for wire pairs in free space. Again we assume for simplification of the formulas that the terminations on both sides of the transmission lines are equal (and drop the source/load subscripts on terminations). Then (25) with low-frequency approximations of inductance and capacitance yields the desired closed-form expressions for near-end crosstalk

$$\gamma_{\mathrm{NE,cap}} \approx \frac{-\pi\varepsilon\left(1+\ln^{-1}\left(\frac{d^2}{ra}\right)\right)}{4\ln^2\left(\frac{a}{r}\right)\left(\frac{1}{R_{d,v}}+\frac{1}{2R_{c,v}}\right)}a^2 j\omega l d^{-2}$$

$$\gamma_{\mathrm{NE,ind}} \approx \frac{-\mu}{4\pi}\left(\frac{1}{R_{d,c}}+\frac{1}{2R_{c,c}}\right)a^2 j\omega l d^{-2}. \tag{28}$$

Again, the sum of inductive and capacitive coupling gives the total NEXT. The relation between crosstalk and all designable

Authorized licensed use limited to: Technical Activities Board. Downloaded on June 23,2020 at 15:17:24 UTC from IEEE Xplore. Restrictions apply.

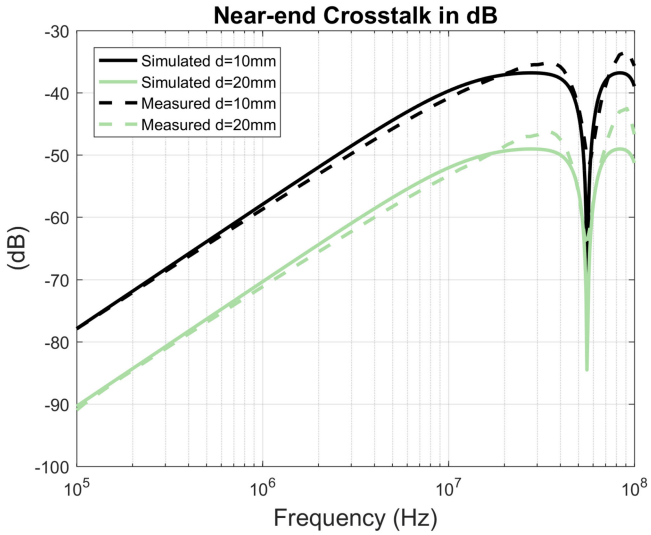

Fig. 6. MTL simulations and measurements of NEXT for two separation distances in the wire configuration given in Fig. 2(b).

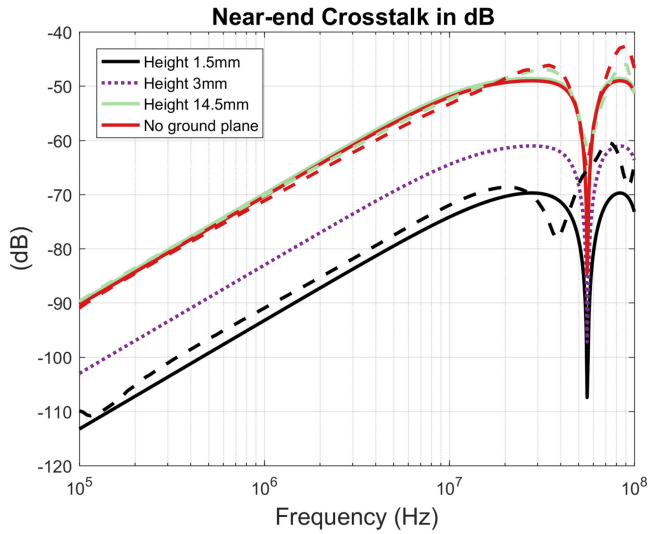

Fig. 7. MTL simulations (solid lines) and measurements (dashed lines) of NEXT for three values of the height above a ground plane in the wire configuration given in Fig. 2(a). For $h = 3$ mm (purple, dotted line) only MTL simulation data is available. One result for the situation without ground plane [Fig. 2(b)] is given (red).

parameters is shown by these equations. The dependency on the separation distance is quadratic, as opposed to the fourth-order behavior of the previous section. This is confirmed by the comparison of two measured and two simulated results for separation distances of 10 mm and 20 mm, as shown in Fig. 6. All simulation parameters are equal to the previous case. The difference in crosstalk between these traces is roughly 12 dB. Moreover, there is again a good match between measurements and MTL simulations.

In addition to separation dependency, Fig. 7 shows MTL simulations and measurements of near-end crosstalk that focus on the height above the ground plane. Results are given for varying heights of wire pairs above a ground plane, as well as for the situation without a ground plane. Measurements and simulations are in good agreement. Moreover, the 12 dB difference between the simulated results for h is 1.5 mm and 3 mm confirms the quadratic dependency found from (24). Finally, both measured and simulated results in Fig. 7 indicate that when moving wire pairs away from the ground plane the crosstalk levels approach those for wire pairs in free space.

C. Parameter Dependencies

Closed-form expressions for low-frequency crosstalk are useful to extract the dependencies of crosstalk on designable parameters. Table I gives an overview of all leading-order dependencies for both inductive and capacitive crosstalk, with a plus or minus sign showing if crosstalk increases or decreases with an increase of the parameter value. The sensitivities have been derived from (24) and (28), which were obtained under the assumption that $a \ll d$, as well as $h \ll d$ in case a ground plane is involved. Specifically, when $2a \leq d$ and $d \geq 2h\sqrt{2}$ hold, nearly all dependencies given in Table I hold. For inductive coupling, these sensitivities are simply read from the exponents in (22) and (28). For capacitive coupling, logarithms complicate the dependencies on a, h, and r. For the case with the ground plane, the logarithm in the denominator of (23) can be simplified when $a \leq 2h$, which is a reasonable assumption when the wires of a pair are separated only by some insulation. In that case, it can be derived that the dependency on height is quadratic. The dependency on intrapair separation is then such that the increase in crosstalk is roughly 5–8 dB when a is doubled, hence the dependency stated by Table I is roughly first-order. Similar intrapair separation dependency holds for the case without a ground plane. Note that when any of the given assumptions is violated, the order of dependency for certain parameters might change. However, the trend of crosstalk behavior with respect to that parameter will usually remain equal.

Clearly, the parameter with the highest sensitivity is the separation distance between two pairs close to a ground plane. Wire radius does not affect the inductive crosstalk at all, while the dependency of capacitive crosstalk still involves a complex logarithm. Therefore, its sensitivity on r is such that crosstalk increases roughly 10 dB when r is doubled, implying slightly more than linear behavior, hence the $>+1$ in the table.

The impedance parameter Z given in Table I refers to the differential mode impedance between either the victim or culprit pair for capacitive or inductive crosstalk, respectively. For both types of crosstalk, the dependency on termination impedances is of order one, but inductive crosstalk is always inversely proportional to culprit terminations, while capacitive crosstalk is linearly dependent on victim impedance.

IV. Nonuniform Transmission Lines

Apart from its use in the derivation of closed-form expressions, the set of equations given in (7) can also be applied to nonuniform transmission lines. For instance, to compute crosstalk in a bundle of twisted pairs the most common solution is to use a sufficient amount of uniform cascaded sections (UCS) and to multiply the chain parameter matrices for each

Authorized licensed use limited to: Technical Activities Board. Downloaded on June 23,2020 at 15:17:24 UTC from IEEE Xplore. Restrictions apply.

TABLE I
NEAR-END CROSSTALK BETWEEN WIRE PAIRS: SENSITIVITY TO MODEL PARAMETERS[1]

GROUND PLANE	TYPE	d	a	h	r	Z	f	ℓ	ε	μ
Yes	Inductive	-4	+2	+2	0	-1	+1	+1	0	+1
Yes	Capacitive	-4	+1*	+2*	>+1	+1	+1	+1	+1	0
No	Inductive	-2	+2	-	0	-1	+1	+1	0	+1
No	Capacitive	-2	+1	-	>+1	+1	+1	+1	+1	0

[1] In general, all orders of dependency hold for $2a \leq d$ and $d \geq h \cdot 2\sqrt{2}$. The only extra assumption is needed for *, in which the complex logarithm of (23) is simplified assuming $a \leq 2h$.

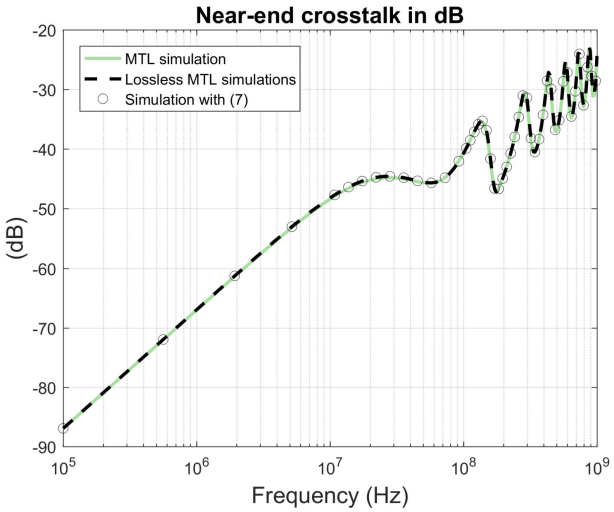

Fig. 8. Simulated NEXT for a bundle of 7 twisted pairs. Results are compared for full MTL simulation (green), lossless MTL simulation and the low-frequency approximation in (7) applied to each uniform segment.

section [2], [3]. Using the exact form of the chain parameter matrices involves performing eigen decompositions for each uniform section. However, each section is usually small in terms of wavelengths. Therefore, when quick computations are desired above the inclusion of high-frequency losses, the approximate low-frequency form (7) can also be used for each segment.

Fig. 8 shows simulation results for a bundle of seven 1 m long twisted pairs that are separated 3.4 mm from each other and are enclosed by a bundle shield. Near-end crosstalk between the center pair and one of the surrounding pairs is considered. More details of this bundle are given in [20]. The results for full MTL simulation including finite wire conductivity ($\sigma = 6e7$ S/m) are compared to those of a lossless MTL simulation and a simulation in which (7) is used for the chain parameter matrices of each uniform section. This approximate result exactly matches that of lossless MTL simulation, while the difference with respect to the full MTL simulation obtains a maximum of only 0.86 dB in the resonance area. The computation time of the full MTL simulation, on a single core of a simple laptop with Intel i5 processor and 8 GB of RAM, is more than 20 times higher than the time needed for the approximate solution, while this is 10 times when compared with the lossless MTL simulation. Therefore, the solution that utilizes (7) forms a better candidate for cable optimizations and early risk assessments than the usual MTL simulations.

V. CONCLUSION

Efficient crosstalk design rules are required to optimize cable bundles and to yield early routing of low-risk signals as well as early risk identification for high-risk signals. We have presented a mathematical methodology to analyse crosstalk in MTLs. With the proposed low-frequency technique closed-form expressions that directly relate crosstalk to designable parameters are derived.

For two cable configurations involving wire pairs close to a perfectly conducting ground plane and in free space, the low-frequency analysis has resulted in expressions for near-end crosstalk that clearly show the differences between all designable parameter sensitivities. For instance, in the configuration with the ground plane, the crosstalk decreases up to 24 dB when the interpair separation distance is doubled. However, when the height of the wire pairs above the ground plane becomes large compared with the interpair separation distance, the crosstalk behavior approaches that of wire pairs in free space. In that case, crosstalk increases with a more familiar 12 dB when doubling the separation distance.

Using the efficient low-frequency approximations of the chain parameter matrices leads to accurate lossless results when analysing more complex nonuniform MTLs with UCS. However, the computation time becomes more than 20 times smaller when compared with the usual MTL simulations. Therefore, in this case, the low-frequency approximations can well be applied to perform a quick analysis of cable bundles that involve twisted pairs, meandering of cables, and other complex nonlinear phenomena.

REFERENCES

[1] C. R. Paul, *Analysis of Multiconductor Transmission Lines*. New York, NY, USA: Wiley, 1994.
[2] C. R. Paul and J. W. McKnight, "Prediction of crosstalk involving twisted pairs of wires – Part I: A transmission-line model for twisted-wires pairs," *IEEE Trans. Electromagn. Compat.*, vol. EMC-21, no. 2, pp. 92–105, May 1979.
[3] C. Jullien, P. Besnier, M. Dunand, and I. Junqua, "Advanced modeling of crosstalk between an unshielded twisted pair and an unshielded wire above ground plane," *IEEE Trans. Electromagn. Compat.*, vol. 55, no. 1, pp. 183–194, Feb. 2013.
[4] J. C. Clements, C. R. Paul, and A. T. Adams, "Computation of the capacitance matrix for systems of dielectric-coated cylindrical conductors," *IEEE Trans. Electromagn. Compat.*, vol. EMC-17, no. 4, pp. 238–248, Nov. 1975.
[5] S. Sun G. Liu, J. L. Drewniak, and D. J. Pommerenke, "Hand-assembled cable bundle modeling for crosstalk and common-mode radiation prediction," *IEEE Trans. Electromagn. Compat.*, vol. 49, no. 3, pp. 708–718, Aug. 2007.

Authorized licensed use limited to: Technical Activities Board. Downloaded on June 23,2020 at 15:17:24 UTC from IEEE Xplore. Restrictions apply.

[6] G. Spadacini, F. Grassi, and S. A. Pignari, "Field-to-wire coupling model for the common mode in random bundles of twisted-wire pairs," *IEEE Trans. Electromagn. Compat.*, vol. 57, no. 5, pp. 1246–1254, Oct. 2015.
[7] G. Spadacini and S. A. Pignari, "Numerical assessment of radiated susceptibility of twisted-wire pairs with random nonuniform twisting," *IEEE Trans. Electromagn. Compat.*, vol. 55, no. 5, pp. 956–964, Oct. 2013.
[8] P. Manfredi, D. De Zutter, and D. Vande Ginste, "Analysis of nonuniform transmission lines with an iterative and adaptive perturbation technique," *IEEE Trans. Electromagn. Compat.*, vol. 58, no. 3, pp. 859–867, Jun. 2016.
[9] Z. Fei, Y. Huang, J. Zhou, and Q. Xu, "Uncertainty quantification of crosstalk using stochastic reduced order models," *IEEE Trans. Electromagn. Compat.*, vol. 59, no. 1, pp. 228–239, Feb. 2017.
[10] M. Wu, D. G. Beetner, T. H. Hubing, H. Ke, and S. Sun, "Statistical prediction of 'reasonable worst-case' crosstalk in cable bundles," *IEEE Trans. Electromagn. Compat.*, vol. 51, no. 3, pp. 842–851, Aug. 2009.
[11] F. Diouf and F. Canavero, "Crosstalk statistics via collocation method," in *Proc. IEEE Int. Symp. Electromagn. Compat.*, Austin, TX, USA, Aug. 2009, pp. 92–97.
[12] D. Bellan and S. A. Pignari, "Efficient estimation of crosstalk statistics in random wire bundles with lacing cords," *IEEE Trans. Electromagn. Compat.*, vol. 53, no. 1, pp. 209–218, Feb. 2011.
[13] S. Salio, F. Canavero, D. Lecointe, and W. Tabbara, "Crosstalk prediction on wire bundles by Kriging approach," in *Proc. IEEE Int. Symp. Electromagn. Compat.*, Washington, DC, USA, Aug. 2002, pp. 197–202.
[14] L. R. A. X. De Menezes, D. W. P. Thomas, C. Christopoulos, A. Ajayi, and P. Sewell, "The use of unscented transforms for statistical analysis in EMC," in *Proc. IEEE Int. Symp. Electromagn. Compat.*, Hamburg, Germany, 2008, pp. 1–5.
[15] C. Jullien *et al.*, "Determination de la diaphonie entre plusieurs harnais complexes au sein d'un avion," in *Proc. Colloque Int.sur la Comp. Electromagn.*, Rennes, France, Jul. 2016. [Online]. Available: https://www.researchgate.net/publication/318882370
[16] D. R. J. White and M. Mardiguian, "Near-field conductor-to-conductor coupling (Crosstalk)," in *EMI Control Methodology and Procedures (Handbook series on electromagnetic interference and compatibility)*, vol. 8. Gainesville, FL, USA: Interference Control Technol., 1989.
[17] C. R. Paul, *Introduction to Electromagnetic Compatibility*. New York, NY, USA: Wiley, 2006.
[18] C. R. Paul and J. W. McKnight, "Prediction of crosstalk involving twisted pairs of wires—Part II: A simplified low-frequency prediction model," *IEEE Trans. Electromagn. Compat.*, vol. EMC-21, no. 2, pp. 105–114, May 1979.
[19] J. H. G. J. Lansink Rotgerink and H. Schippers, "Crosstalk modelling of unshielded wire pairs," in *Proc. IEEE Int. Symp. Electromagn. Compat.*, Gothenburg, Sweden, 2014, pp. 641–646.
[20] J. H. G. J. Lansink Rotgerink and F. Leferink, "A crosstalk sensitivity analysis on bundles of twisted wire pairs," in *Proc. IEEE Int. Symp. Electromagn. Compat.*, Amsterdam, The Netherlands, 2018, pp. 11–16.

Jesper Lansink Rotgerink (M'17) received the B.Sc. (*cum laude*) and M.Sc. (*cum laude*) degrees in applied mathematics from the University of Twente, Enschede, The Netherlands, in 2010 and 2013, respectively.

Since 2013, he has been working with the Netherlands Aerospace Centre, Marknesse, The Netherlands, where his main fields of interest are aerospace EMC, specifically crosstalk between cables, as well as propagation of EM waves through radomes and its effect on antenna performance, radar absorbing materials and antennas for aerospace.

Harmen Schippers (M'01) received the Ph.D. degree in applied mathematics from the University of Technology Delft, Delft, The Netherlands, in 1982.

Since 1981, he has been a Senior Scientist with the Netherlands Aerospace Centre, Marknesse, The Netherlands. He has research experience in addressing computational methods for aeroelastic, aeroacoustic, and electromagnetic challenges. His current research interests include the development of technology for integrating smart antennas into aircraft structures and the development of computational tools for the analysis of antennae installed on aircraft and spacecraft.

Frank Leferink (M'91–SM'08) received the B.Sc., M.Sc., and Ph.D. degrees, all in electrical engineering, from the University of Twente, Enschede, The Netherlands, in 1984, 1992, and 2001, respectively.

He has been with THALES, Hengelo, The Netherlands, since 1984, where he is the EMC Technical Authority. In 2003, he was appointed as a (part-time, full research) Professor and the Chair for EMC at the University of Twente. He has authored or coauthored more than 200 peer-reviewed papers.

Dr. Leferink is the Chair of the IEEE EMC Benelux Chapter, a member of the Board of Directors of the IEEE EMC Society, a member of ISC EMC Europe, and an Associate Editor of the IEEE TRANSACTIONS ON ELECTROMAGNETIC COMPATIBILITY.

Authorized licensed use limited to: Technical Activities Board. Downloaded on June 23,2020 at 15:17:24 UTC from IEEE Xplore. Restrictions apply.